C. R. Chimie 18 (2015) 979–985

Contents lists available at ScienceDirect

Comptes Rendus Chimie

www.sciencedirect.com

Full paper/Mémoire

A novel organic–inorganic hybrid compound based on Anderson-type polyoxometalates and anthranilamide

Safa Thabet, Brahim Ayed *, Amor Haddad

Département de chimie, laboratoire de matériaux et cristallochimie, faculté de science, rue Environnement, 5000 Monastir, Tunisia

ARTICLE INFO

Article history:
Received 21 March 2015
Accepted after revision 23 June 2015
Available online 29 August 2015

Keywords:
Hybrids material
Polyoxometalates
Anderson-B anion
X-ray diffraction
Photoluminescent property

ABSTRACT

A new organic-inorganic hybrid material, $(C_7H_9N_2O)_2[Al(OH)_7Mo_6O_{17}]\cdot 12H_2O$ (**1**), was prepared and characterized by elemental analysis, IR and UV–visible spectroscopies, TG–DTA analysis, and single-crystal X-ray diffraction. The title compound crystallizes in the triclinic system, space group $P\bar{1}$ with $a = 10.237(2)$ Å, $b = 10.415(1)$ Å, $c = 10.545(1)$ Å, $\alpha = 87.27(1)^\circ$, $\beta = 102.17(1)^\circ$, $\gamma = 95.24(1)^\circ$, $Z = 1$. Single-crystal X-ray analysis shows that compound (**1**) possesses a 3D framework, which is built up of Anderson polyoxoanions, organic cations and water molecules; the extensive net hydrogen bonds between cations and anions contribute to the crystal packing. Furthermore, the luminescent property of (**1**) in the solid state was investigated.

1. Introduction

The polyoxometalates (POMs), as a class of transition-metal oxide clusters, possess remarkable features of metal oxide surfaces and various geometry topologies, which make them attractive in applications in fields as diverse as catalysis, magnetism, photochemistry, electrochemistry, material science, and medicine [1–7]. Recently, these fascinating molecular aggregates were broadly used as inorganic segments to support organic derivatives [8,9] or metal–organic complexes in the assembly of inorganic–organic hybrid materials [10].

To date, many hybrid organic–inorganic compounds have been reported, by selecting the appropriate POMs as building blocks, such as Wells–Dawson, Keggin, Lindquist, and Silverton-type POMs [11–14]. Anderson's POMs possess planar structures and each addenda atom has two terminal oxygen atoms with high reactivity, which provide diverse possibilities of intermolecular linkages. Therefore, many such compounds implying this type of polyoxoanions with several types of cationic organic species have been successfully explored, such as adenine [15], histidine [16], phenanthroline [17], glycine [18] and pyridine-3-carboxylic acid [19]. Herein, we used anthranilamides as linker agents in a new hexamolybdoaluminate extended structure, which has not been reported before, to our knowledge.

This work focuses on the study of the crystal structure and the luminescent properties of $(C_7H_9N_2O)_2[Al(OH)_7Mo_6O_{17}]\cdot 12H_2O$ (**1**), and on the characterization of this material.

2. Experimental

2.1. Materials and general methods

All reagents were purchased commercially and used without further purification. The infrared spectra were recorded as KBr pellets, in the 4000–400 cm^{-1} range, using a Nicolet 470 FTIR spectrophotometer. The UV–visible absorption spectrum was recorded on a PerkinElmer

* Corresponding author.
E-mail addresses: thabet_safa@yahoo.com (S. Thabet), brahimayed@yaoo.fr (B. Ayed).

http://dx.doi.org/10.1016/j.crci.2015.06.020
1631-0748/

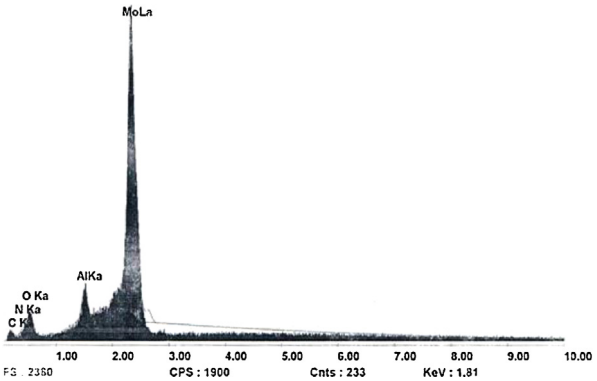

Fig. 1. EDAX patterns of the compound (**1**).

Lambda 19 spectrophotometer. A Setaram TG–DTA92 thermo-analyzer was used to perform thermal treatments on samples of the title compound. The TG-DTA thermograms were obtained with 14.43 mg of material. The samples were placed in an open platinum crucible and heated in air at a 10 °C/min heating rate; an empty crucible was used as a reference. The photoluminescence spectra were measured using a PerkinElmer spectrophotometer (LS 55) with a xenon lamp.

2.2. Chemical preparation

The title compound was prepared by mixing 20 mL of an aqueous solution of $Na_2MoO_4{\cdot}2H_2O$ (1 mmol) with 10 mL of an aqueous solution of $Al(NO_3)_9{\cdot}9H_2O$ (0.7 mmol). The pH of the resulting cloudy solution was adjusted to 3.7 by adding nitric acid (4 M). When the color of the reaction turned clear, 2-aminobenzamide (0.8 mmol) was added. The obtained solution was left to evaporate slowly at room temperature. After a few days, the colorless block crystals were formed and the yield was 60% based on Mo. A qualitative energy-dispersive spectroscopy (EDS) analysis of some crystals on a JEOL-JSM 5400 scanning electron microscope revealed the presence of Al, Mo, O, N and C elements (Fig. 1). Elem. Anal. Found: Mo, 37.65; Al, 1.63; C, 13.87; H, 3.15; N, 3.54; (%). Calcd: Mo, 38.97; Al, 1.83; C, 11.38; H, 2.87; N, 3.79 (%).

2.3. X-ray crystallography

The structure was determined from single-crystal X-ray diffraction data, collected at room temperature using an Enraf-Nonius CAD-4 diffractometer using monochromated Mo Kα radiation (λ = 0.71069 Å); A total of 4072 independent reflections ($1.96° < \theta < 24.97°$) were recorded, of which 3844 reflections were considered ($R_{int} = 0.025$). Compound (**1**) crystallizes in the triclinic system with space group $P\bar{1}$. All calculations were performed using the WinGX crystallographic software package [20]. The data were solved and refined using SHELX-97 [21]. The positions of molybdenum and aluminum were obtained using the Patterson heavy atom method, and successive Fourier analysis allowed the other atoms to be located. All hydrogen atoms were fixed from difference Fourier and were refined isotopically, but some H atoms attached to water molecules could not be located and were directly included in the final molecular formula. A final refinement cycle using all atomic positions and including anisotropic displacement parameters led to the reliability factors $R_1 = 0.045$ and $wR_2 = 0.123$.

Table 1
Crystal structure data for **1**.

Crystal data	
Formula/formula weight	$C_{14}H_{42}N_4O_{38}AlMo_6$/1477.14 g·mol^{-1}
Crystal system	Triclinic
Space group/*Z*	$P\bar{1}$/1
Lattice parameters	$a = 10.237(1)$ Å, $\alpha = 87.278(1)°$ $b = 10.415(1)$ Å, $\beta = 102.176\ (1)°$ $c = 10.545(1)$ Å, $\gamma = 95.248(1)°$
Volume	$V = 1094{,}12(3)$ Å^3
Density (calculated) (g/cm^3)	2.242
Absorption coefficient μ (mm^{-1})	1.803
F(000)	733
Size (mm^3)/color	0.22 × 0.18 × 0.13/colorless
Intensity measurement	
Diffractometer	Enraf-Nonius_*CAD4*
Monochromator	Graphite
Wavelength, Mo Kα	λ = 0.71073 Å
Temperature	293
Theta range	1.96°/24.97°
h, *k*, *l* range	−12/11, −12/12, 0/12
No. of independent reflections	3844
Structure determination	
Unic reflections included: ($I > 2\sigma I$)	3596
Programs used	SHELX-97
No. of refined parameters	288
Goodness-of-fit on F^2	1.054
R (anisotropic)	0.0450
R_w (anisotropic)	0.124
Extinction coefficient	0.0056(9)
$\Delta\rho_{min}/\Delta\rho_{max}$ (e/Å^3)	1.752/−1.832
Largest shift/error	0.001

The recording conditions and crystallographic data are reported in Table 1. Selected bond lengths of **1** are listed in Table 2. The structural graphics were created by DIAMOND program [22].

3. Results and discussion

3.1. Structure description

Single-crystal X-ray diffraction analysis reveals that the hybrid compound (**1**) is built of $\mathbf{[Al(OH)_7Mo_6O_{17}]^{2-}}$ heteropolyoxoanions (abbreviated as {$AlMo_6$}), 2-aminobenzamide cations, and isolated water molecules. The unit cell of (**1**) is shown in Fig. 2.

From a general point of view, the hybrid structure may be described as a succession of alternating organic and inorganic sheets along the *b*-direction. A purely inorganic (noted A) sheet was built from water molecules and $[Al(OH)_7Mo_6O_{17}]^{2-}$ anionic clusters. The second (noted B) is formed by 2-aminobenzamide cations that are organized in opposition around the inversion center, as shown in Fig. 3. To the best of our knowledge, no analogous 3D

Table 2
Selected bond lengths (Å) of **1**.

Mo1-O11	1.6845(2)	Mo3-O10	1.6882(5)
Mo1-O12	1.7130(5)	Mo3-O8	1.6942(4)
Mo1-O4	1.9366(2)	Mo3-O4^{i1}	1.9214(2)
Mo1-O5	1.9645(3)	Mo3-O6	1.9763(7)
Mo1-O2	2.2861(2)	Mo3-O3^{i1}	2.2940(3)
Mo1-O1	2.3367(7)	Mo3-O2^{i1}	2.3044(5)
Mo2-O9	1.7057(3)	Al -O1	1.9091(1)
Mo2-O7	1.7090(2)	Al -O1^{i1}	1.9091(2)
Mo2-O5^{i1}	1.90585(1)	Al -O2	1.8965(5)
Mo2-O6^{i1}	1.9679(5)	Al -O2^{i1}	1.8965(1)
Mo2-O3	2.2667(2)	Al -O3	1.8957(3)
Mo2-O1^{i1}	2.3071(6)	Al-O3^{i1}	1.8957(7)
Organic groups			
C1-C2^{i1} = 1.3843(2)			
C2-C3^{i2} = 1.3922(3)		C6-C1-C2 = 121.60(5)	
C2- C7^{i3} = 1.5044(6)		N1-C1-C6 = 116.84(4)	
C3-C4^{i1} = 1.3934(5)		N1-C1-C2 = 121.35(4)	
C4-C5^{i4} = 1.3775(1)		C7-C2-C3 = 120.62(4)	
C5-C6 = 1.3760(2)		C7-C2-C1 = 120.46(4)	
C6-C1 = 1.3828(3)		C2-C3-C4 = 119.40(5)	
C1- N1^{i5} = 1.4622(4)		C3-C4-C5 = 120.26(6)	
C7-N2^{i6} = 1.3243(4)		C4-C5-C6 = 120.86(5)	
C7-O13 = 1.2289(2)		C5-C6-C1 = 118.61(4)	

i1 $-x, -y, -z+1$; i2 $x+1, y+1$, i3 $x-1, y, z$; i4 $-x+1, -y+1, z+1$; i5 $x, y, z+1$; i6 $x, y+1, z$.

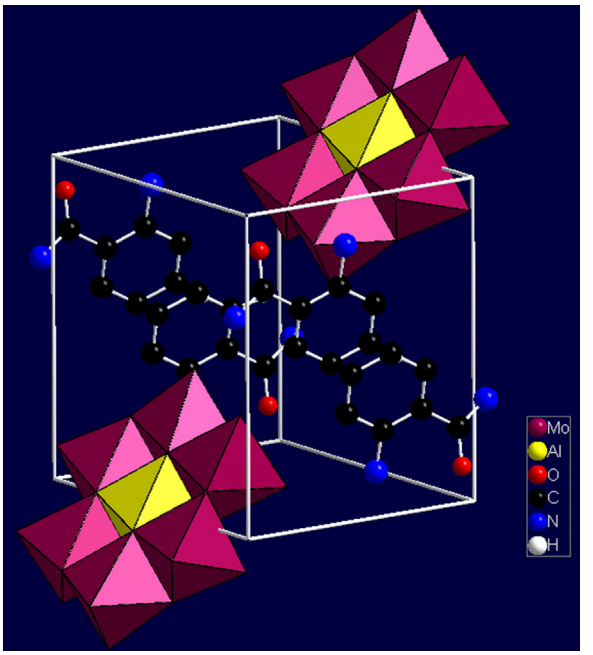

Fig. 2. (Color online.) The unit cell of compound (**1**). The hydrogen atoms and crystal water molecules are omitted for clarity.

structure consisting of Anderson-type POM building blocks and anthranilamide bases have been reported in the literature.

The polyoxoanion {$AlMo_6$} belongs to the B-type Anderson structure, which consists of seven edge-sharing octahedra, six of which are {MoO_6} octahedra, arranged hexagonally around the central {$Al(OH)_7$} octahedron. All molybdenum sites present an octahedral coordination geometry with different distortion extents. The Mo atoms are shifted toward the direction of the terminal oxygen atoms away from the centers of the octahedra. This behavior is as well reflected by Mo–O bond distances. In fact, the Mo–O bonds in {$AlMo_6$} can be divided into three types:

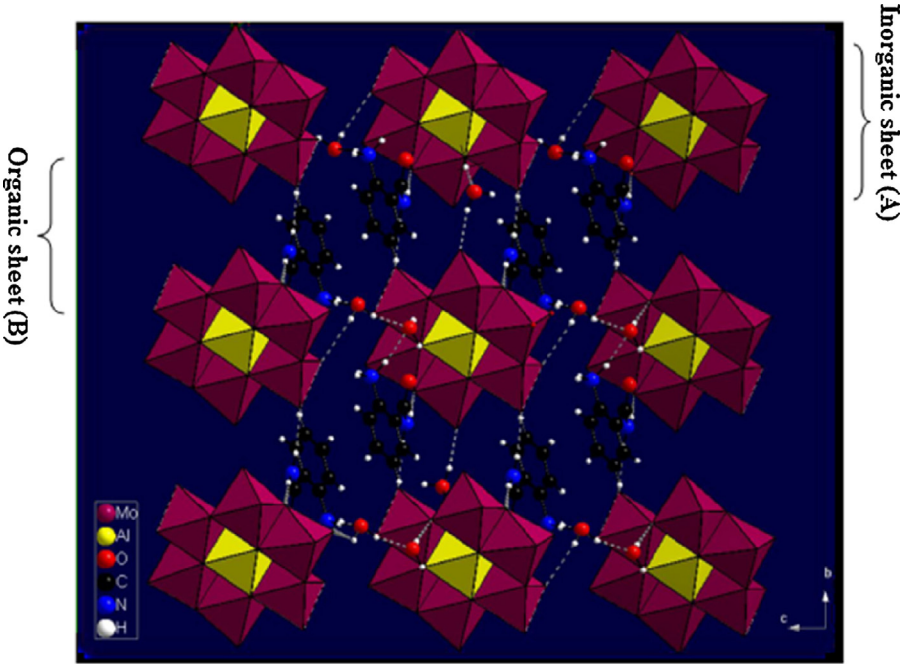

Fig. 3. (Color online.) View of the three-dimensional network of compound (**1**) along the *a*-axis.

- molybdenum–triply bridging oxygen bonds, in which the central oxygen connects two Mo atoms and the aluminum atom with an Mo–Oc distance of 2.265(3)–2.336(2) Å;
- molybdenum–doubly bridging oxygen bonds with an Mo–Ob distance of 1.905(3)–1.975(3) Å;
- molybdenum–terminal oxygen bonds, in which the oxygen is linked to one Mo atom with an Mo–Ot distance of 1.683(6)–1.713(3) Å.

The Mo–Mo distances lie in the 3.310(2)–3.338(2) Å range. In the crystal structure, the central Al–O distances vary from 1.895(6) to 1.909(1) Å. The bond angles of O–Al–O_{cis} range from 83.96(2) to 96.19(2) and O–Al–O_{trans} is 180°. Selected bond distances within the {$AlMo_6$} unit of the hybrid compound are listed in Table 2 and are in accordance with the values for {$AlMo_6$}-based compounds reported elsewhere [23–27].

BVS calculations [28,29] revealed that all the molybdenum atoms have valence sums ranging from 5.768 to 5.864, with an average value of 5.811, close to the ideal value of 6 for Mo^{VI}. The calculated average value of aluminum (+III) atoms is 2.816. The sum of the bond valence about the O atoms is estimated to be close to 2, the largest deviations being 1.110, 1.175, 1.202 and 1.624 for the triply bridging oxygen atoms around the Al^{3+} ion and a bridging oxygen atom (O6), respectively. On the other hand, as shown in Table 2, the Mo2—O6, Mo3—O6 bond distances are shown to be the longest among the Mo—Ob bond distances. Therefore, we presume that the H^+ ions in the polyanion might be bound to these four oxygen atoms, yielding the calculated framework charge of $[Al(OH)_7Mo_6O_{17}]^{2-}$ [30,31].

In the present atomic arrangement (**1**), there are multipoint directional hydrogen bond interactions among $[Al(OH)_7Mo_6O_{17}]^{2-}$ heteropolyoxoanion, 2-aminobenzamide cation, and lattice water in the range of 2.709–3.241 Å (Table 3). Of the 24 oxygen atoms in the hexamolybdoaluminate anion, 12 take part in the construction of an hydrogen-bonding supramolecular network. As shown in Fig. 4, the Anderson-type polyanions are interlinked together via water molecules through hydrogen bonds to generate a two-dimensional network in the plane (*ab*). Furthermore, the layers extend into a 3D-dimensional supramolecular framework also by hydrogen bond interactions. It is interesting that this organization along the axis *c* creates cavities to which the anthranilamide cations were encapsulated inside and well surrounded by these units (Fig. 5).

The anthranilamide cations, acting as charge-compensating cations, are stacked approximately face-to-face to

Table 3
Selected hydrogen bonds.

D–H···A	D–H (Å)	H···A (Å)	D···A (Å)	D–H···A (°)
O1–H1···OW2^{i1}	0.819	2.010	2.820	170.13
O2–H3···OW1	0.812	1.905	2.709	170.90
O3–H3···O13	0.951	1.682	2.625	170.71
N1–H8···O9	1.013	1.941	2.856	148.82
N1–H9···OW3^{i2}	0.928	1.965	2.879	168.51
N1–H10···OW4	1.069	1.740	2.805	173.78
N2–H11···O7	0.941	3.036	2.097	174.94
N2–H12···O4^{i3}	0.897	2.190	3.079	170.54
OW1H1W1···OW2	0.936	1.832	2.744	164.11
OW1H2W1···OW3	0.851	2.041	2.751	140.43
OW2H1W2···O12	0.923	1.916	2.812	163.23
OW2H2W2···OW5	0.842	2.008	2.822	162.15
OW3H1W3···O5	0.858	1.933	2.777	167.24
OW3H2W3···O13	0.965	2.456	3.290	144.51
OW4H1W4···O9	0.828	2.399	3.170	155.18
OW4H1W4···O8	0.828	2.471	2.918	114.88
OW4H2W4···OW3	0.928	1.913	2.814	162.87
OW4-H1W4···O10^{i4}	0.828	2.633	3.147	121.67
OW5H1W5···OW6	0.980	2.347	2.958	119.70

i1 $-x, -y+1, -z+1$; i2 $x-1, y, z-1$; i3 $x, y-1, z$; i4 $-x-1, -y, -z+1$.

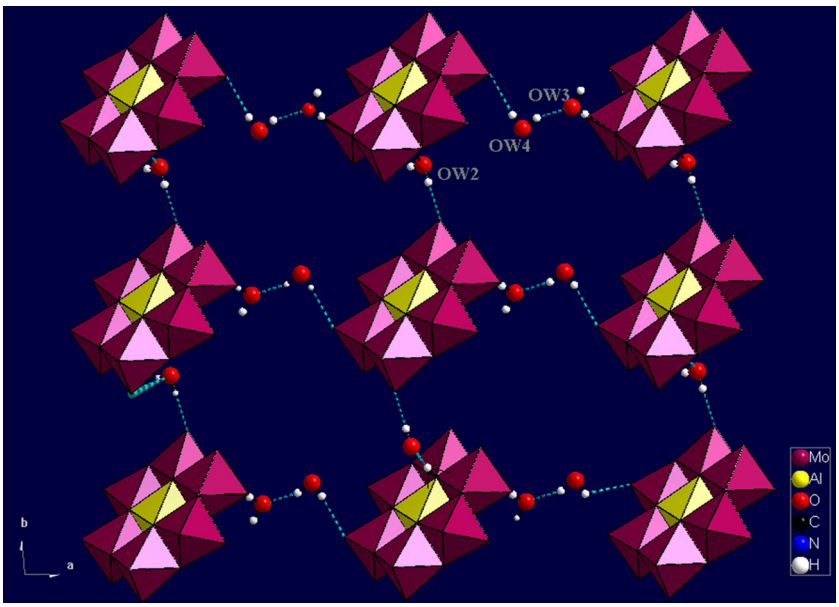

Fig. 4. (Color online.) Two-dimensional grid-like network constructed of $[Al(OH)_7Mo_6O_{17}]^{2-}$ anions with water molecules viewed along the *c*-axis.

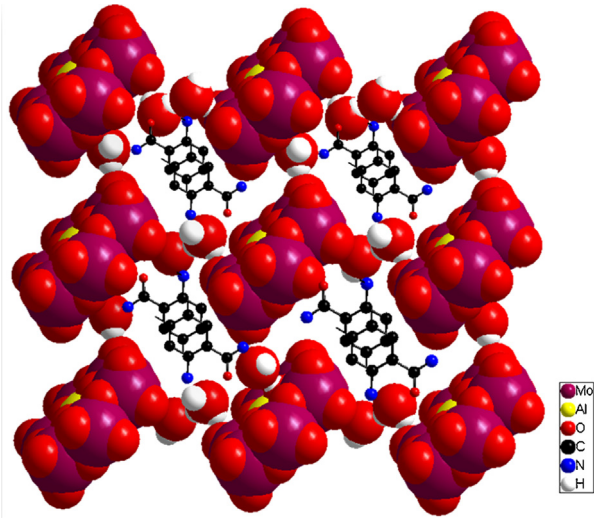

Fig. 5. (Color online.) Space-filling diagram of the 3-D network and the cavities constructed from $[Al(OH)_7Mo_6O_{17}]^{2-}$anions encircling the anthranilamide cations,shown in a ball-and-stick representation.

form columns. The centroid–centroid distances between the nearest-neighbor cation rings are 3.709(9) Å. The shortest interplanar distance, which is much shorter than 3.80 Å, indicates the formation of π–π interactions. It is believed that the extensive hydrogen-bonding interactions and π–π interactions play an important role in stabilizing the three-dimensional supramolecular network.

3.2. IR absorption spectroscopy

The vibrational spectrum exhibits the characteristic bands associated with the building constituents from which title material was synthesized: the polyoxoanion $[Al(OH)_7Mo_6O_{17}]^{2-}$, the anthranilamide cations, and water molecules.

The characteristic absorptions of the $[Al(OH)_7Mo_6O_{17}]^{2-}$ polyanions appear below 1000 cm^{-1}. A medium band at 773 cm^{-1} was characteristic of the stretching frequency of Al–O. One can see the absorptions bands at 960, 888 and 682 cm^{-1} may be assigned to the stretching vibrations of the Mo–Ot and Mo–Ob and Mo–Oc bonds, respectively [19,32,33]. Furthermore, the presence of the anthranilamide moiety is suggested by the occurrence of a series of vibrational bands at 3280, 3175, 2800, 2620, 2364, 1730, 1531, 1480, 1330, and 1235 cm^{-1} (Fig. 6). A broad absorption, observed in the region between 3175 and 2364 cm^{-1}, can be assigned to the N–H and C–H stretching modes. The stretching and bending modes of the NH_3^+ groups appear via the medium band at 3280 cm^{-1} and the strong band at 1531 cm^{-1}, respectively. Absorption at 1730 cm^{-1} is attributed to the stretching vibrations of the carbonyl group. The bands from 1235 to 1531 cm^{-1} can be assigned to the bending vibrations C–C and C–N of the aromatic ligand [16,17]. On the other hand, the title compound exhibit bands at the 3428 and 1660 cm^{-1}, corresponding to the stretching and bending vibrations of the OH groups of the water molecules, respectively.

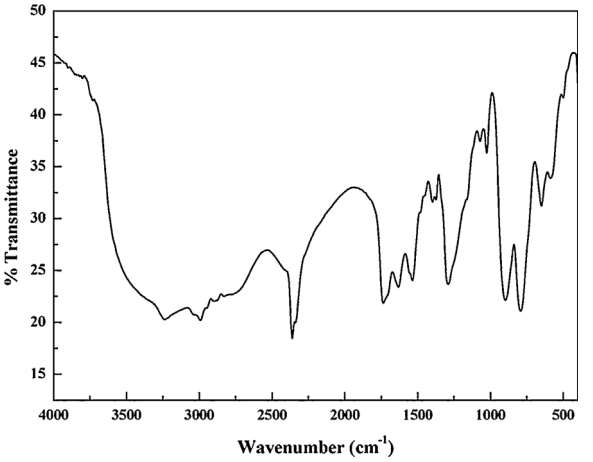

Fig. 6. IR spectrum of compound (**1**).

3.3. UV–visible spectra

As shown in Fig. 7, the UV spectrum of compound (**1**) in aqueous solution displays two absorption peaks at 217 nm and 270 nm, respectively. The spectral band of higher energy can be assigned to the charge-transfer transition of Ot → Mo, whereas the spectral band of lower energy can be attributed to the $O_{b,c}$ → Mo charge transition [34–36]. The limit value of absorption is 310 nm, indicating an optical energy gap (E_g) of 3.97 eV, which allows us to classify this polyanion among the insulators.

3.4. Thermal behavior

Fig. 8 shows both TG and DTA thermograms of compound (**1**). The TG curve of the title compound exhibits four weight loss steps; the first three steps of weight loss 6.33%, 4.24% and 5.93% (calc. 6.09%, 3.23%, 5.49%), observed in the temperature range from 50 to 262 °C, are ascribed to the release of all lattice water molecules. In this domain, the DTA curve reveals a succession of endothermic peaks located at 70, 129 and 242 °C. The different types of interactions for the water molecule in the network explain the departure of the water molecule in this large

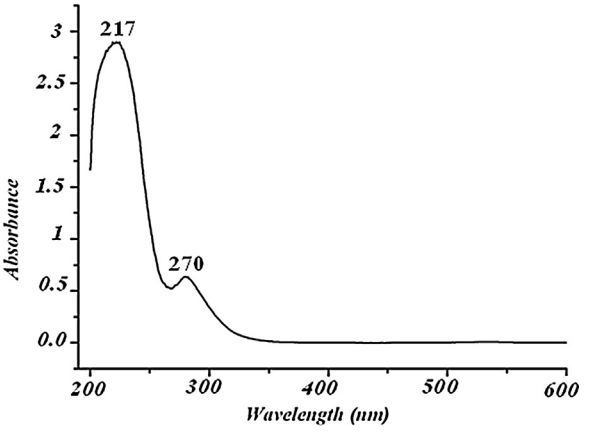

Fig. 7. UV spectrum of title material (**1**).

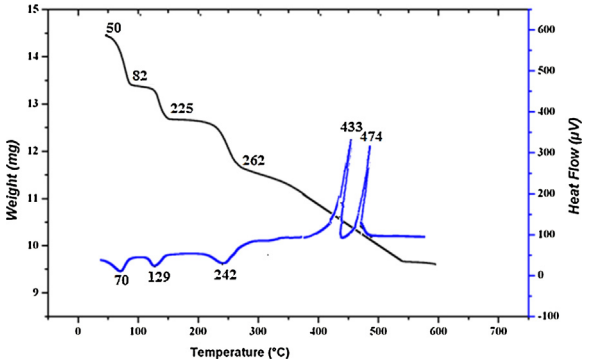

Fig. 8. TG–DTA thermograms of compound (**1**).

temperature range. The decomposition of the anthranilamidinum cations arises in the fourth step between 262 and 550 °C with a weight loss of 16.21% (calc. 18%). This pyrolysis is stated, in the DTA curve, by two exothermic peaks at 433 °C and 474 °C.

3.5. Luminescence property

The luminescence properties of POM-based supramolecular compounds have been extensively explored for their diverse functionalities and applications in lighting, display, sensing, and optical devices [37–40]. Therefore, luminescent investigations of the anthranilamide ligand and compounds (**1**) in the solid state have been carried out at room temperature.

As illustrated in Fig. 9, the emission spectrum of compound (**1**) shows an intense emission maximum at 422 nm and other shoulder peaks at 462, 483, 529, 576 and 619 nm (λ_{ex} = 320 nm). Compared with 2-aminobenzamide luminescence, which is well known (λ_{ex} = 320 nm, λ_{em} = 420 nm), it is possible that the emission of the title compound (**1**) originates from the anthranilamide ligand and should be attributed to a mixture characteristic of intraligand and ligand-to-ligand charge transitions. In addition, this result is comparable to those obtained with other compounds implying several aromatic organic ligands [41,42,19,43].

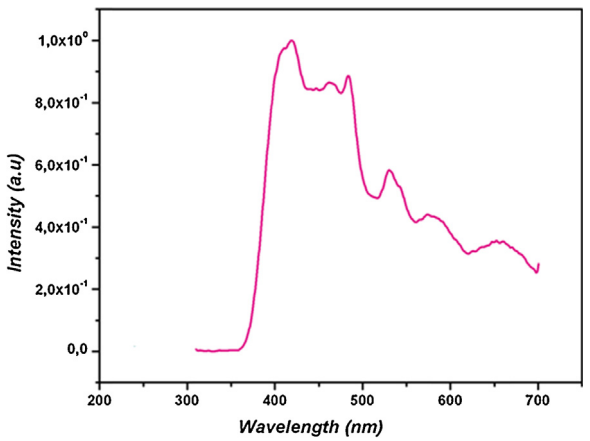

Fig. 9. Emission spectrum of compound (**1**) in the solid state at room temperature (λ_{ex} = 320 nm).

4. Conclusion

In summary, we have successfully synthesized a new inorganic–organic hybrid, based on $[Al(OH)_7Mo_6O_{17}]^{2-}$ Anderson-type polyanion and 2-aminobenzamide ligand, by slow evaporation at room temperature. The crystal structure of the title compound has been elucidated by X-ray crystallography and confirmed by elemental analysis, IR, UV and TG–DTA. The new hybrid material exhibits a porous 3-D hydrogen-bonded host framework with channel-encapsulated anthranilamide cation. Luminescent information on compound (**1**) exhibits an emission peak maximum at 441 nm, which can be assigned to the photoluminescence signal of the 2-aminobenzamide ligand. It is hoped that more organic-inorganic hybrid compounds with mixed ligands will be synthesized by choosing different kinds of ligands and POMs.

Acknowledgment

This work was supported by the Ministry of Higher Education and Scientific Research of Tunisia.

Appendix A. Text

The crystallographic data for the structure reported in this paper have been deposited with the Cambridge Crystallographic Data Center under CCDC Number 1043478. Copies of the data can be obtained free of charge on application to CCDC, 12 Union Road, Cambridge CB2 1EZ, UK, fax: +44 1223 336 033, email: deposit@ccdc.cam.ac.uk; or on the web: http://www.ccdc.cam.ac.uk.

References

[1] M.T. Pope, Heteropoly and isopolyoxometalates, Springer, New York, 1983.
[2] C.L. Hill, C.M. Prosser-McCartha, Coord. Chem. Rev. 143 (1995) 407.
[3] M.H. Alizadeh, H. Razavi, F.F. Bamoharram, Kinet. Catal. 44 (2003) 524.
[4] M.T. Pope, A. Muller (Eds.), Polyoxometalates: From Platonic Solids to Anti-retroviral Activity, Kluwer Academic Publishers, Dordrecht, The Netherlands, 1994.
[5] R. Khoshnavazi, H. Eshtiagh-Hosseini, M.H. Alizadeh, M.T. Pope, Inorg. Chim. Acta 360 (2007) 686.
[6] M.H. Alizadeh, A.R. Salimi, Spectrochim. Acta A 65 (2006) 1104.
[7] A.J. Gaunt, I. May, M. Helliwell, S. Richardson, J. Am. Chem. Soc. 124 (2002) 13350.
[8] I.A. Razak, S. Raj, S. Chantrapromma, H.K. Fun, Y.S. Zhou, X.Z. You, J. Chem. Crystallogr. 31 (2001) 255.
[9] N. Legagneux, E. Jeanneau, J.-M. Basset, F. Lefebvre, J. Mol. Struct. 921 (2009) 300.
[10] H. Ma, L. Gong, F. Wang, X. Wang, Struct. Chem. 19 (2008) 435.
[11] (a) Y. Lu, Y. Xu, E.B. Wang, J. Lu, L. Xu, Cryst. Growth Des. 5 (2005) 257; (b) F. Bonhomme, J.P. Larentzos, M. Nyman, Inorg. Chem. 44 (2005) 1774; (c) M. Vasylyeva, R. Popovitz-Birob, R. Neumanna, J. Mol. Struct. 656 (2003) 27.
[12] (a) J. Niu, D. Guo, J. Wang, J. Zhao, Cryst. Growth Des. 4 (2004) 241; (b) Y. Lu, Y. Xu, Y. Li, E. Wang, X. Xu, Y. Ma, Inorg. Chem. 45 (2006) 2055.
[13] P.J. Hagrman, D. Hagrman, J. Zubieta, Angew. Chem. Int. Ed. 38 (1999) 3165.
[14] C.D. Wu, C.Z. Lu, H.H. Zhuang, J.S. Huang, J. Am. Chem. Soc. 124 (2002) 3836.
[15] S. Thabet, B. Ayed, A. Haddad, Bull. Mater. Sci. 37 (2014) 1503.
[16] S. Thabet, B. Ayed, A. Haddad, Mater. Res. Bull. 47 (2012) 3791.
[17] H. Maa, L. Wub, H. Pang, X. Meng, J. Peng, J. Mol. Struct. 967 (2010) 15.

[18] H. An, Y. Guo, Y. Li, E. Wang, L. Xu, C. Hu, Inorg. Chem. Commun. 7 (2004) 521.
[19] H. An, T. Xu, C. Jia, H. Zheng, W. Mu, J. Mol. Struct. 933 (2009) 86.
[20] L.J. Farrugia, WinGX-version 1.63, J. Appl. Crystallogr. 32 (1999) 837.
[21] G.M. Sheldrick, Acta Crystallogr. A 64 (2008) 112.
[22] K. Brandenburg, DIAMOND Visual Crystal Structure Information System, 1997.
[23] H.Y. An, Y.G. Li, E.B. Wang, C.Y. Sun, L. Xu, J. Mol. Struct. 743 (2005) 117.
[24] H.Y. An, Y.Q. Guo, E. Wang, L. Xu, C.G. Hu, Inorg. Chem. Commun. 7 (2004) 521.
[25] H.Y. An, D.R. Xiao, E. Wang, Y.G. Li, L. Xu, J. Mol. Struct. 751 (2005) 184.
[26] Y. Zhou, J. Yin, L. Zhang, J. Mol. Struct. 920 (2009) 61.
[27] B. Gao, S.X. Liu, L.H. Xie, M. Yu, C.D. Zhang, C.Y. Sun, H.Y. Cheng, J. Solid State Chem. 179 (2006) 1681.
[28] I.D. Brown, D. Altermatt, Acta Crystallogr. B 41 (1985) 244.
[29] Softbv web page by Pr. Stefan Adams. http://www.kristall.uni.mki.gwdg.de/softbv.
[30] R. Cao, S. Liu, L. Xie, Y. Pan, J. Cao, Y. Ren, L. Xu, Inorg. Chem. 46 (2007) 3541.
[31] U. Lee, Acta Crystallogr. E63 (2007) i5.
[32] Y. Liu, S. Liu, H. Ji, S. Zhang, L. Cai, R. Cao, J. Cluster Sci. 20 (2009) 535.
[33] M. Yu, B. Gao, D. Liang, J. Cluster Sci. 25 (2014) 377.
[34] T. Yamase, Chem. Rev. 98 (1998) 307.
[35] H.Y. An, T.Q. Xu, E. Wang, C.G. Meng, Inorg. Chem. Commun. 10 (2007) 1453.
[36] X.M. Zhang, B.Z. Shen, X.Z. You, H.K. Fun, Polyhedron 16 (1997) 95.
[37] X.J. Wang, Y.H. Liu, H.W. Hou, Y.T. Fan, Cryst. Growth Des. 12 (2012) 2435.
[38] W. Kana, S. Wena, Y. Kana, H. Hua-You, X. Niua, Zhanga, Synth. Met. 198 (2014) 51.
[39] K. Binnemans, Chem. Rev. 109 (2009) 4283.
[40] S.V. Eliseeva, J.C.G. Bunzl, Chem. Soc. Rev. 39 (2010) 189.
[41] B. An, R. Zhou, L. Sun, Y. Bai, D. Dang, Mol. Biomol. Spect. 128 (2014) 319.
[42] I. Nagazi, A. Haddad, J. Clust. Sci. 25 (2014) 627.
[43] S. Zhang, Y. Li, Y. Liu, R. Cao, C. Sun, H. Ji, S. Liu, J. Mol. Struct. 920 (2009) 284.